Delft University of Technology

Improved Numerical Method for Aw-Rascle Type Continuum Traffic Flow Models

Mohammadian, Saeed; van Wageningen-Kessels, Femke

Important note
To cite this publication, please use the final published version (if applicable).
Please check the document version above.

Improved Numerical Method for Aw-Rascle Type Continuum Traffic Flow Models

Saeed Mohammadian[*]

School of Civil Engineering & Built Environment

Science & Engineering Faculty

Queensland University of Technology

2 George St, GPO Box 2434

Brisbane QLD 4001, Australia

saeed.mohammadian@hdr.qut.edu.au

Femke van Wageningen-Kessels

Assistant Professor

Department of Logistics, Tourism and Services Management

Faculty of Business and Economics

German University of Technology in Oman (GUtech)

femke.vanwageningen@gutech.edu.om

Department of Transport & Planning

Delft University of Technology

Faculty of Civil Engineering and Geosciences

Delft, the Netherlands

f.l.m.vanwageningen-kessels@tudelft.nl

* Corresponding Author

Word Count: 5389 word texts + 7 table/figures x250 (each) = 7148

`

1   **Abstract**

2   Continuum traffic flow models are essentially nonlinear hyperbolic systems of Partial
3   Differential Equations (PDEs). Except for limited specific cases, these systems must be solved
4   numerically in general. Mathematical structure of continuum models can be different for each
5   class of models. As a result, suitable numerical schemes for some classes of models may not be
6   efficient for others. In this study, an improved numerical method is proposed for a class of second-
7   order traffic flow models. The method is based on McCormack scheme, which is a widely-used
8   method for non-homogeneous second-order traffic flow models, but fails to produce reasonable
9   results for homogeneous models including Aw-Rascle type models which are the focus of this
10 paper. It is shown that this is mainly due to spurious numerical oscillations. Smoothing methods
11 to overcome these issues are studied and applied. Central Dispersion (CD) and Artificial Viscosity
12 (AV) methods are incorporated to the standard McCormack scheme and tested. To reduce
13 numerical diffusion, a Total Variation Diminishing (TVD) Runge-Kutta time stepping scheme is
14 applied. Results show the capability of the proposed methods - and especially the AV to eliminate
15 the oscillations of the standard McCormack scheme as well as controlling numerical diffusion.

16 **Keywords:** Traffic flow, continuum models, Aw-Rascle model, Zhang model, McCormack
17 scheme, numerical method

18   **Introduction**

19 Traffic flow modelling has attracted growing research attention due to the need for
20 optimizing the usage of either existing or future road infrastructure. The increasing and dynamic
21 nature of demand on urban networks and the environmental, societal and economic costs
22 associated with traffic jams are some reasons justifying robust studies of traffic flow, results of
23 which could be advantageous in decision-making process of traffic control strategies. Dynamic
24 non-linear phenomena such as stop-and-go waves and synchronization in congestion [1] require
25 models that are able to reproduce them, while keeping the number of parameters limited [2].
26 Furthermore, computer predictions should be acceptably accurate and computational costs have
27 to remain low when simulations are applied to real-world traffic scenarios.

28 Various techniques have been employed for traffic state estimation over the past decades
29 including mathematical modelling [3]. Continuum (macroscopic) approaches along with car-
30 following and cellular automata models are the most successful methods for mathematical study
31 of traffic flow. For detailed reviews of traffic flow models, we refer the reader to [4-8]. In this
32 study, we focus on continuum models because of their low computational costs, simpler
33 calibration compared to other approaches, and their high potential for incorporation in traffic
34 control strategies [9]. Continuum models reproduce the behavior of traffic flow by modelling it as
35 a fluid, with aggregated variables such as average speed and average density. First-order
36 continuum models assume that local speed is always in equilibrium with local density, while
37 second-order continuum models define a dynamic equation for local speed [10]. In general,
38 second-order models can allow traffic states to fluctuate over equilibrium states introducing
39 acceleration behavior and its associate phenomena such as reaction time and anticipation. Such
40 fluctuations have been also associated with some complex phenomena such as traffic oscillations,
41 hysteresis, and capacity drop which have been observed in empirical traffic studies [11]. For a
42 detailed review of such phenomena, we refer the reader to [12-16]. One of the privileges of
43 second-order models is their ability to capture such nonlinear traffic phenomena, which cannot
44 be reproduced by single-class first-order models [7]. However, complex mathematical structure
45 of such models, call for different numerical schemes to first-order models [6].

46 Second-order continuum traffic flow models are classified as non-linear system of
47 hyperbolic equations [17]. In the presence of a source term, they are also classified as non-
48 homogeneous equations. The Payne-Witham [18, 19], Kerner-Konhäuser [20] and the gas-kinetic
49 based [21] models are examples of non-homogeneous second-order traffic flow models because
50 they include a relaxation acceleration source. However, in some other continuum models such as
51 the Aw-Rascle model [22] and the Zhang model [23] there is no source term and they are classified

`

1 as homogeneous equations. Some non-homogeneous models do not satisfy the anisotropy
2 conditions [24, 25], which means driver do not react to their follower in traffic flow. However,
3 homogeneous Aw-Rascle and Zhang models have favorable properties such as anisotropic
4 behavior and it can be proven that solutions to important initial value problems exist [26] .

5   One of the most common frameworks for solving non-homogeneous continuum models is
6 to use McCormack method because of its simplicity, limited computational costs and little
7 associated numerical diffusion [27]. Furthermore, the minimum supply demand method, which is
8 commonly used for first order models, has been adapted for second-order traffic flow models [28].
9 In the context of hyperbolic systems, high-order methods have been proposed for Computational
10 Fluid Dynamics and heat transfer applications [17, 29]. By translating concepts from such studies,
11 some complex methods have also been proposed for continuum traffic flow models [30, 31].
12 However, the McCormack still remains one of the most commonly-used schemes in traffic flow
13 modelling and simulation [6]. As a second-order scheme, McCormack scheme provides less
14 numerical diffusion compared to first-order schemes [3]. However, this scheme is associated with
15 numerical oscillations. When applied to non-homogeneous models, numerical oscillations can be
16 dispersed due to effect of source terms. Therefore, results are usually only slightly affected by
17 numerical oscillations [27]. However, due to lack of source terms, this scheme fails to reproduce
18 plausible results for the homogeneous models, as we will show in Section 4.

19 The contribution of this research is to adapt the McCormack scheme to be able to reproduce
20 reasonable results when applied to homogeneous second-order traffic flow models, such as the
21 Aw-Rascle model. Therefore, two smoothing methods are studied: the Central Dispersion
22 Smoothing (CS) [32] and the Artificial Viscosity (AV) [33]. In order to increase order of temporal
23 accuracy, total Variation Diminishing Runge-Kutta time stepping [34] is also added to the method.
24 Various numerical experiments are performed to evaluate the ability of improved scheme.

25 The rest of the paper is organized as follows: In Section 2, the applied traffic flow models are
26 introduced. The numerical methods, including McCormack scheme and smoothing methods are
27 covered in the Section 3. In Section 4, test cases are introduced and their results are discussed.
28 Finally, some concluding remarks complete the study in section 5.

29 ## Continuum traffic flow models

30 The general formulation of a second-order traffic flow model in conservative form is as follows
31 [10]:

$$\partial_t U + \partial_x F(U) = S(U) \tag{1}$$

32 where vector U indicates state variables, usually ρ the local density of vehicles (veh/m) and v the
33 local macroscopic speed $\left(\frac{m}{s}\right)$. $F(U)$ is the flux function and $S(U)$ is the source term which can
34 represent relaxation or anticipation. The system is non-homogeneous when the source term $S(U)$
35 is nonzero. Payne-type and Gas-kinetic based traffic models [19, 21] are classified as non-
36 homogenous models. The system in (1) can be written in quasi-linear form as follows:

$$\partial_t U + J(U)\partial_x U = S(U) \tag{2}$$

37 where $J(U) = \frac{\partial F}{\partial U}$ is the Jacobian matrix. Characteristic speeds equal the eigenvalues of the system
38 and can be obtained by solving $det[J(U) - \lambda I] = 0$ for the eigenvalues λ. In the presence of
39 distinct and real characteristic speeds, the system is hyperbolic. Characteristic speeds can be
40 studied to see if the model preserves the anisotropic nature of the traffic flow [24, 25].

41 *Aw-Rascle type traffic flow model*

42 Aw-Rascle type of traffic flow models represent a generic family of homogenous and anisotropic
43 higher-order traffic flow models. For a section of road without on-ramps and off-ramps, Aw-Rascle
44 type models can be written in the following formulation [22]:

$$\begin{cases} \partial_t \rho + \partial_x(\rho v) = 0 \\ \partial_t \rho(v + P(\rho)) + \partial_x(\rho v(v + P(\rho))) = 0 \end{cases} \qquad (3),$$

1 where v is vehicle speed (in m/s) and $P(\rho)$ is an increasing function of density to guarantee that
2 the model is anisotropic and can be written as:

$$P(\rho) = C_0^2 \rho^\gamma - \psi \qquad (4),$$

3 where C_0 is sonic velocity, ψ is a constant to regulate pressure, and γ is always greater than zero.
4 The system has two real eigenvalues: $\lambda_1 = v - \rho P'(\rho)$ and $\lambda_2 = v$. Furthermore, except for at
5 zero density ($\rho = 0$), the eigenvalues are distinct and thus the system is strictly hyperbolic.

6 *Zhang model*

7 Zhang model is a special case of the Aw-Rascle type of models [23], in which the dynamic speed
8 function is derived from a microscopic car-following model, leading to the following pressure
9 function:

$$P(\rho) = -v_e(\rho) \qquad (5),$$

10 where $v_e(\rho)$ is the equilibrium speed-density function, in this case Greenshields' model [35]:

$$v_e(\rho) = v_{max}\left(1 - \frac{\rho}{\rho_{jam}}\right) \qquad (6),$$

11 with v_{max} representing the maximum vehicle speed and ρ_{jam} is the jam density.

12 **Numerical methods**

13 In this section, the proposed numerical methods for solving Aw-Rascle type models are discussed.
14 The McCormack method with smoothing is applied for spatial integration. Temporal integration
15 is done using a Total Variation Diminishing (TVD) Runge-Kutta scheme.

16 *McCormack scheme*

17 The McCormack scheme (see e.g. [36]) is a second-order finite difference method that has been
18 applied successfully to non-homogeneous higher order traffic flow models [27]. It consists of a
19 predictor and a corrector step:

20 Predictor

$$U_i^{n+1/2} = U_i^n - \frac{dt}{dx}(F_i^n - F_{i-1}^n) \qquad (7),$$

21 Corrector

$$U_i^{n+1} = 0.5\left(U_i^n + U_i^{n+\frac{1}{2}}\right) - 0.5\frac{dt}{dx}\left(F_{i+1}^{n+1/2} - F_i^{n+1/2}\right) \qquad (8),$$

22 As will become clear in Section 4, the standard McCormack method induces oscillations and is not
23 suitable for homogeneous models such as Aw-Rascle type of models. Therefore, smoothing is
24 applied. Two different smoothing methods are studied, as described in the following.

25 *3.2 Central Dispersion method*

26 The first method for smoothing, the Central Dispersion Smoothing (CD) method [36], is
27 implemented on the updated results in the McCormack:

$$U_{i(CDS)}^{n+1} = (1 - S).U_i^{n+1} + S\left(\frac{U_{i+1}^{n+1} + U_{i-1}^{n+1}}{2}\right) \qquad (9),$$

28 where S is a weight factor and $0 \leq S \leq 1$. With $S = 0$ there is no smoothing at all and the method
29 reduces to the standard McCormack scheme. This method, in fact, acts as a hybrid scheme since
30 it computes the traffic state as weighted average of results by McCormack method and Lax-
31 Friedrichs scheme (see e.g. [36]). When choosing $S = 1$, the Lax-Friedrichs scheme substitutes the
32 second step of McCormack scheme as:

`

$$U_i^{n+1} = 0.5(U_{i-1}^n + U_{i+1}^n) + 0.5\frac{dt}{dx}(F_{i+1}^n - F_{i-1}^n)$$

(10)

1 However, since Lax-Friedrichs scheme is diffusive [36], taking values for S close to 1 results in
2 considerable numerical diffusion. In the test cases, a proper value for S was established by trial
3 and error.

4 At the boundaries, U_{i+1}^{n+1} or U_{i-1}^{n+1} does not exist and smoothing is performed through:

$$U_{i(CD)}^{n+1} = (1-S).U_i^{n+1} + S\left(\frac{U_{i+1}^{n+1} + U_i^{n+1}}{2}\right)$$

(11)

or

$$U_{i(CD)}^{n+1} = (1-S).U_i^{n+1} + S\left(\frac{U_i^{n+1} + U_{i-1}^{n+1}}{2}\right)$$

(12)

5 *Artificial Viscosity method*

6 The second smoothing method that we study is the artificial viscosity method (AV) [33]. With
7 AV, the updated results in the McCormack scheme become:

$$U_{i(AV)}^{n+1} = U_i^{n+1} + \varphi_{i+\frac{1}{2}}(U_{i+1}^{n+1} - U_i^{n+1}) - \varphi_{i-\frac{1}{2}}(U_i^{n+1} - U_{i-1}^{n+1})$$

(13),

8 where $\varphi_{i+\frac{1}{2}}$ is the artificial viscosity at $(i+\frac{1}{2})$:

$$\varphi_{i+\frac{1}{2}} = \kappa.max(\varphi_i, \varphi_{i+1})$$

(14),

9 with κ representing the viscosity parameter and φ_i computed as follows:

$$\varphi_i = \frac{|U_{i+1} - 2U_i + U_{i-1}|}{|U_{i+1}| + 2|U_i| + |U_{i-1}|}$$

(15),

10 The technique is similar to adopting flux-liming terms in high-order Total Variation Diminishing
11 (TVD) Lax-Wendroff methods [17] and as discussed in section 4, can provide robust results.

12 At the boundaries, U_{i+1} or U_{i-1} does not exist and the artificial viscosity is computed using:

$$\varphi_i = \frac{|U_{i+1} - U_i|}{|U_{i+1}| + |U_i|}$$

(16),

13

$$\varphi_i = \frac{|U_i - U_{i-1}|}{|U_i| + |U_{i-1}|}$$

(17),

14 *Temporal integration*

15 To achieve higher order of temporal accuracy while avoiding numerical oscillations, a Total
16 Variation Diminishing (TVD) Runge-Kutta scheme [34] is applied for temporal integration. At each
17 time step, the new state variables are approximated as follows:

$$\begin{cases} U^{(p)}_i = U^{(n)}_i + \xi\left(U^{(n)}_i\right) \\ U^{(q)}_i = 3/4U^{(n)}_i + 1/4U^{(p)}_i + 1/4dt\xi\left(U^{(p)}_i\right) \\ U^{(n+1)}_i = 1/3U^{(n)}_i + 2/3U^{(q)}_i + 2/3dt\xi\left(U^{(q)}_i\right) \end{cases}$$

(18),

18 where $U^{(n)}_i$ the state in the i-th grid cell at time step n. p and q can be interpreted as intermediate
19 time steps, used to compute the state $U^{(n+1)}_i$ in the i-th grid cell, at the next time step $n+1$.
20 Furthermore, we use the change rate of effective flux:

$$\xi\left(U^{(n)}\right) = -\frac{dt}{dx}(F_i^n - F_{i-1}^n)$$

(19),

21

`

$$\xi(U^{(n)}) = -\frac{dt}{dx}(F_i^n - F_{i-1}^n) \qquad (20),$$

1 *CFL condition*

2 In order to avoid numerical instabilities, the grid cell and time step size must satisfy the CFL
3 condition:

$$C_r = \max(\lambda_1, \lambda_2)\frac{dt}{dx} \qquad (21),$$

4 with C_r being the CFL number and $\max(\lambda_1, \lambda_2)$ representing the greater propagation speed.
5 Numerical diffusion is lowest when the CFL number is close to 1, see e.g. [37]. In the Aw-Rascle
6 type models, the maximum of eigenvalues equals the maximum speed, is greater than backward
7 propagation speed. In the numerical tests, the parameter values are chosen as in Table 1.

8 ## Numerical tests and discussions

9 In this section, numerical tests are performed for evaluation of proposed numerical
10 methods for application on Aw-Rascle and Zhang models [22, 23]. The model' parameters take
11 values given in Table 1. Test cases differ in their initial conditions. They were chosen to reflect a
12 wide range of realistic traffic scenarios, while also being demanding for the numerical methods.
13 To confine effects of additional source terms, all test cases are performed on homogeneous road
14 of length L. At the boundaries, the following conditions are applied:

$$U_1^n = U_2^n$$
$$U_I^n = U_{I-1}^n \qquad (22),$$

15 where I, denotes the last cell.

16 *Table- 1 Physical and numerical parameters used for Aw-Rascle and Zhang models*

Parameter	Value	Model
Length of road (L)	$12000m$	Both
Maximum speed (v_{max})	$30m/s$	Both
Maximum density (ρ_{jam})	$0.15veh/m$	Both
C_0^2	$80\ m^2/s^2$	Aw-Rascle
ψ	$31.94\ veh.m/s\string^2$	Aw-Rascle
γ	0.5	Aw-Rascle
Critical Density (ρ_{cr})	$0.04veh/m$	Aw-Rascle
Critical Density (ρ_{cr})	$0.075veh/m$	Zhang
S	0.01	Both
κ	0.25	Both
dt	1	Both
dx	$31.7m$	Both
$\max(\lambda_1, \lambda_2)$	$30m/s$	Both
C_r	0.975	Both
dt (Reference solution)	$0.0625s$	Both
dx (Reference Solution)	$1.8m$	Both

17

18 *Case 1) Free-flow traffic with transition from high to low densities*

$$\rho(x,0) = \begin{cases} 0.46\rho_{jam} & for\ x < \frac{L}{2} \\ 0.1\rho_{jam} & for\ x > \frac{L}{2} \end{cases}$$
$$v(x,0) = v_e(\rho(x,0)) \qquad (23),$$

19

Case 2) Congested traffic with transition from high to low densities

$$\rho(x,0) = \begin{cases} 0.9\rho_{jam} & for\ x < \frac{L}{2} \\ 0.55\rho_{jam} & for\ x > \frac{L}{2} \end{cases} \tag{24},$$

$$v(x,0) = v_e(\rho(x,0))$$

Case 3) Queue dissolution

$$\rho(x,0) = \begin{cases} 0.1\rho_{jam} & for\ x \le L/3 \\ \rho_{jam} & for\ L/3 < x \le 2L/3 \\ & for\ L/3 > 2L/3 \\ 0.1\rho_{jam} & \end{cases} \tag{25},$$

$$v(x,0) = v_e(\rho(x,0))$$

Case 4) Free-flow traffic with uniform density and non-equilibrium speeds

$$\rho(x,0) = 0.35\rho_{jam}$$

$$v(x,0) = \begin{cases} v_e(\rho(x,0)) + 5 & for\ x < L/5 \\ v_e(\rho(x,0)) & for\ L/5 < x < 2L/5 \\ v_e(\rho(x,0)) + 5 & for\ x > 2L/5 \end{cases} \tag{26},$$

Case 5) Uniform density with non-equilibrium speeds

$$\rho(x,0) = 0.75\rho_{jam}$$

$$v(x,0) = \begin{cases} v_e(\rho(x,0)) + 5 & for\ x < L/3 \\ v_e(\rho(x,0)) & for\ L/3 < x < 2L/3 \\ v_e(\rho(x,0)) + 5 & for\ x > 2L/3 \end{cases} \tag{27},$$

Case 1-3 include equilibrium traffic states that cannot be simulated through standard McCormack scheme. This is due to either existence of sharp transition from congestion to free-flow regime or formation of them due to oscillatory behavior of the method. In cases 5, 6, initial non-equilibrium traffic states results in formation and propagation of contact discontinuity and expansion waves. Non-convergent formation of numerical oscillations in these cases result in failure of standard McCormack scheme which ultimately lead to physically unrealistic results.

Numerical results for standard McCormack scheme and discussion

In this section, behavior of standard McCormack scheme for simulation of Aw-Rascle type models will be investigated. We apply the method for some test cases, to illustrate why this scheme is not well-suited for this type of problems. Failure in these cases, implies that the method would not work well in any of the other cases either. Afterwards, we test both smoothing methods on all test cases. The standard McCormack scheme is applied to Zhang model, only for test case 1 and 2. Results are illustrated in figure 1.
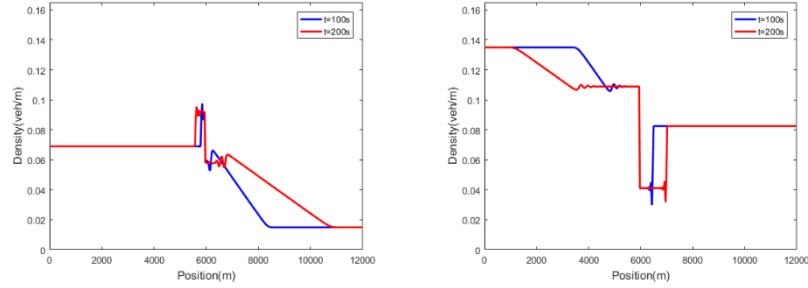
Fig 1) Results of McCormack scheme for transition from higher densities to the lowers in uniform traffic condition. (Left) Case 1, free-flow condition, (Right) Case 2, congestion regime.

Results show oscillations around the transitions from high to low densities. These oscillations lead to discontinuous transitions from congestion to free-flow regime and ultimately results in failure of the method. This is because the Aw-Rascle type models are highly nonlinear and lack a dissipative term to smooth out numerical oscillations that are introduced by the McCormack scheme. Analogous behavior of the McCormack scheme has been reported when the scheme is applied to the shallow water equations with initial sharp transition from subcritical to supercritical flows, in the absence of a dissipative (friction-type) term or in the presence of a booster (topography-type) term for oscillations. We refer the reader to [38, 39] for further discussion on shallow water equations. For this type of problems, smoothing methods are commonly applied to eliminate or reduce oscillations [40, 41]. It should be mentioned that the McCormack scheme can be well-suited for other traffic flow simulations, such as for non-homogeneous models and for specific cases with other initial conditions such as red-light modelling. However, it is not suitable to simulate wide range of realistic traffic scenarios using a homogeneous second-order model.

Set up of numerical tests on smoothed McCormack with TVD Runge-Kutta scheme

Artificial Viscosity (AV) and Central Dispersion (CD) Smoothing methods are applied to decrease the oscillations inherent to the standard McCormack scheme. The smoothing parameters are shown in Table 1. Several values were tested and these turned out to give good results in terms of removing spurious oscillations, while keeping numerical diffusion low. Figure 2 illustrates an example of various smoothing parameters for both AV and CD methods. Choice of Zero smoothing parameters in both methods reduces proposed method to standard McCormack, which cannot provide reasonable solution. It is clear from figure 2 that with the increase in smoothing parameters, numerical diffusion also increase which result in sooner propagation of traffic density. More elaborate testing would be beneficial for future applications. Results are compared with a reference solution that is obtained using a fine grid, with parameters as in Table 1. For the reference solution, AV with the same parameters in accordance with first order explicit time stepping was used. The grid cell sizes are chosen such that the CFL number is equal to the CFL number of the methods on the normal grid. It is worth mentioning that exact solution for discussed models cannot be calculated using techniques such as method of characteristics [17], variational theory [42], or Hamilton-Jacobi representation [43]. In fact, discussed models are both second-order and nonlinear and exact solution for such models cannot be obtained through analytical methods. However, we use fine-grid reference solutions through which our results are evaluated.
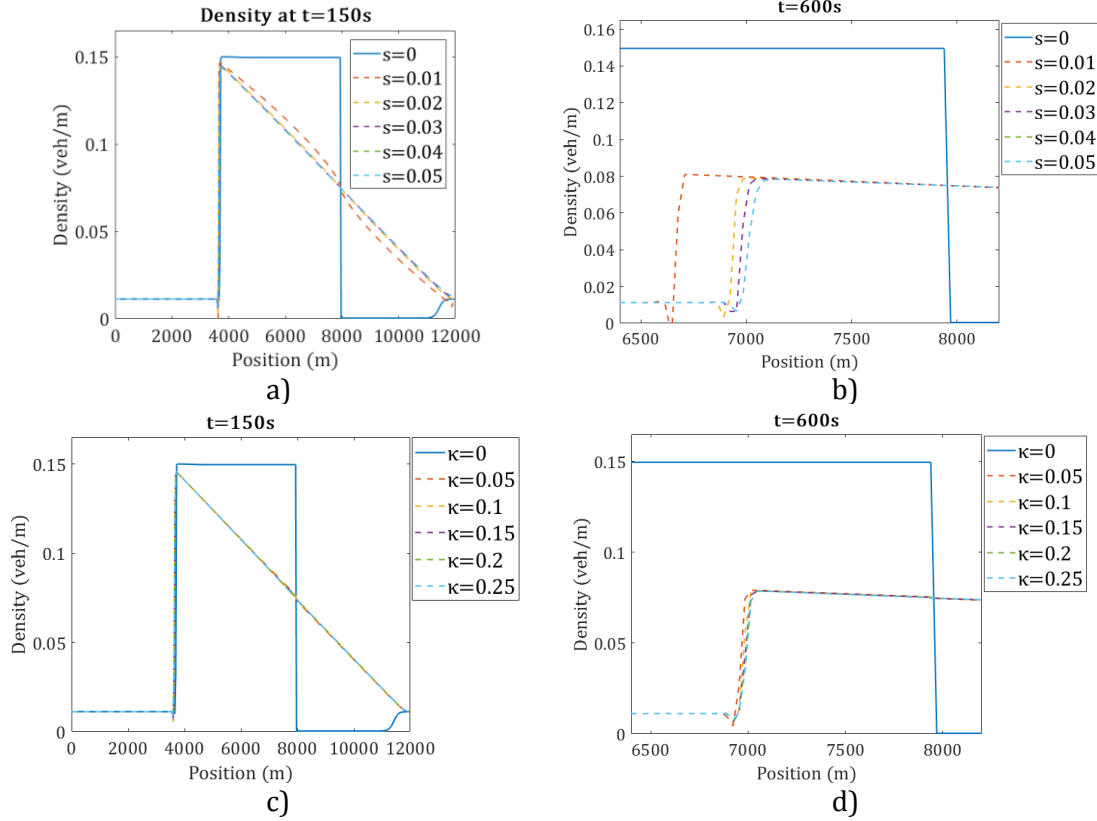
Fig 2- *Effects of choice of smoothing parameter on numerical diffusion for case 3, initial queue problem: a, b) CD method, c, d) AV method*

a) Aw-Rascle model b) Aw-Rascle model c) Aw-Rascle model d) Aw-Rascle model

a) Zhang model b) Zhang model c) Zhang model d) Zhang model
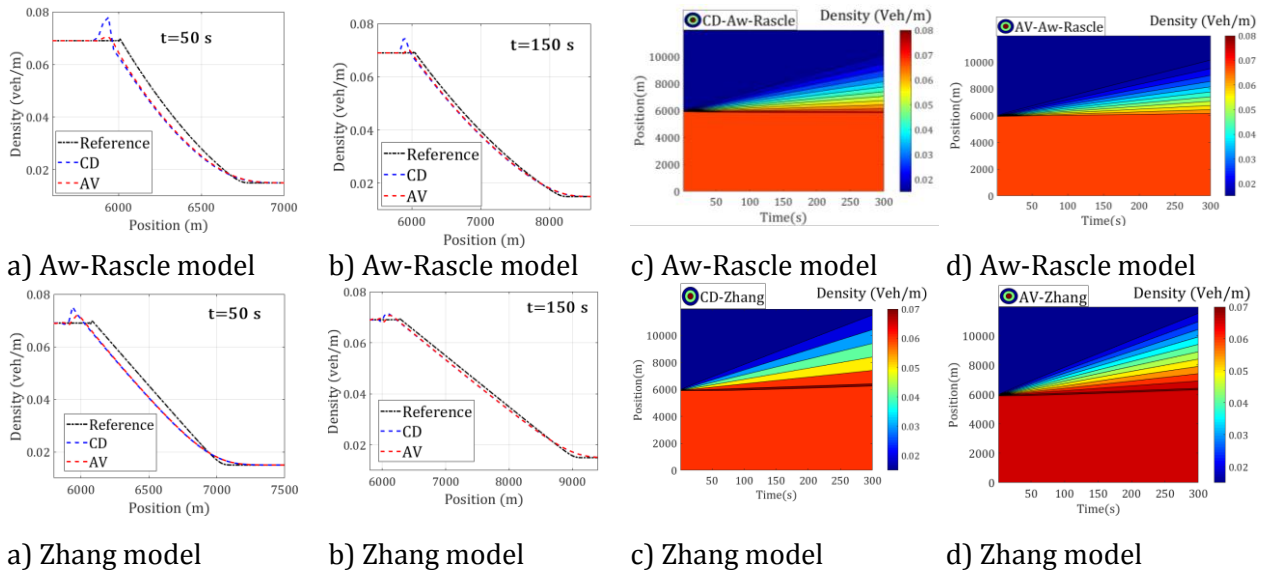
Fig 3) *Results for case 1. a) Cross section at t=50s, b) Cross section at t=150s, c) CD spatiotemporal evolution of local densities, d) AV spatiotemporal evolution of local densities., e) cross section at t=50s, f) Cross section at t=150s, g) CD spatiotemporal evolution of local densities, h) AV spatiotemporal evolution of traffic densities.*

Solution of Riemann problem to the Case 1 is the formation and propagation of expansion waves to the right. This is because initial traffic state is of free-flow regime and the upstream density is greater than that of downstream. Density profile propagates in a slower rate for Aw-Rascle model than for Zhang model because of different parameters taken for traffic pressure functions. As previously stated, McCormack scheme can successfully simulate such cases. However, when the upstream density is very close to critical density, spurious oscillation lead to unreasonable results.

1 Results from figures 3 and 4 clearly show that smoothing methods can overcome previously
2 mentioned problem of standard McCormack method and results. Furthermore, spatiotemporal
3 evolution of density for both Zhang and Aw-Rascle model reveal that overall results provided by
4 these smoothing methods are correct and only on a certain trajectory (the edge of the initial
5 discontinuity) some trivial oscillations can be observed. These slight oscillations are also
6 alleviated more effectively when AV is applied.

a) Aw-Rascle model   b) Aw-Rascle model   c) Aw-Rascle model   d) Aw-Rascle model

a) Zhang model   b) Zhang model   c) Zhang model   d) Zhang model
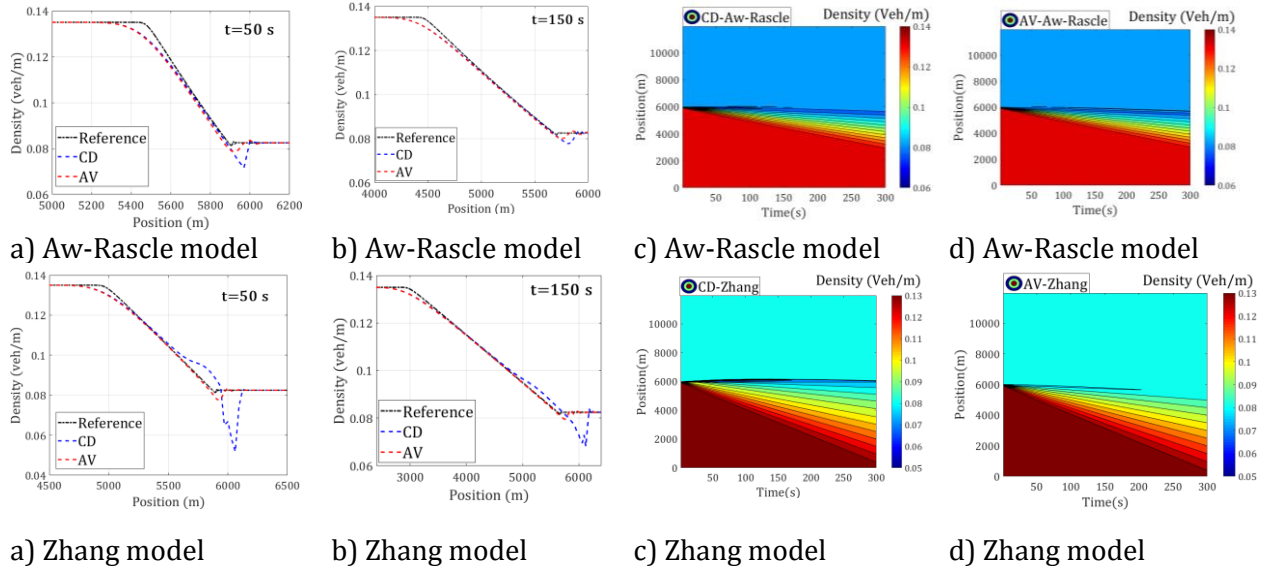
7 Fig 4) *Results case 2. a) Cross section at t=50s, b) Cross section at t=150s, c) CD spatiotemporal*
8 *evolution of local densities, d) AV spatiotemporal evolution of local densities. Results for e) Cross*
9 *section at t=50s, f) Cross section at t=150s, g) CD spatiotemporal evolution of local densities, h) AV*
10 *spatiotemporal evolution of traffic densities.*

11 Being analogous to case one, the second case is also on transition from higher to lower densities.
12 However, due to the dominance of congestion regime characteristic speeds- which determine the
13 direction of traffic waves- are of negative signs and traffic density propagates leftward. Similarly,
14 for the densities close enough to critical density, standard McCormack provides physically absurd
15 results. According to fig- 5, 6, overall results obtained from the two smoothing methods are highly
16 acceptable compared to the reference solution. Although the general propagation of traffic density
17 is correct for each of the smoothing methods, for Zhang model, obtained results from CD method
18 are riddled with greater oscillations on the trajectory following by the edge of the discontinuity.
19 This is because downstream density for Zhang model is closer to its critical density compared to
20 Aw-Rascle model due to its different pressure function. AV smoothing provides less oscillatory
21 results in this case as well. Yet, CD method also provides acceptable results.

a) Aw-Rascle model   b) Aw-Rascle model   c) Aw-Rascle model   d) Aw-Rascle model
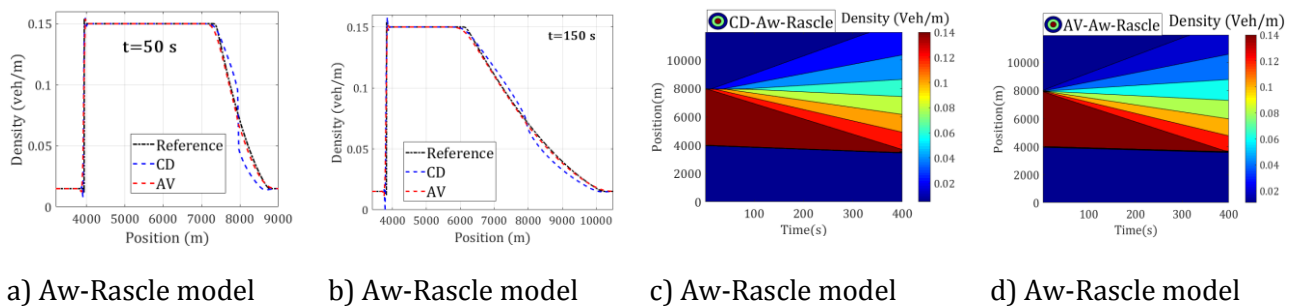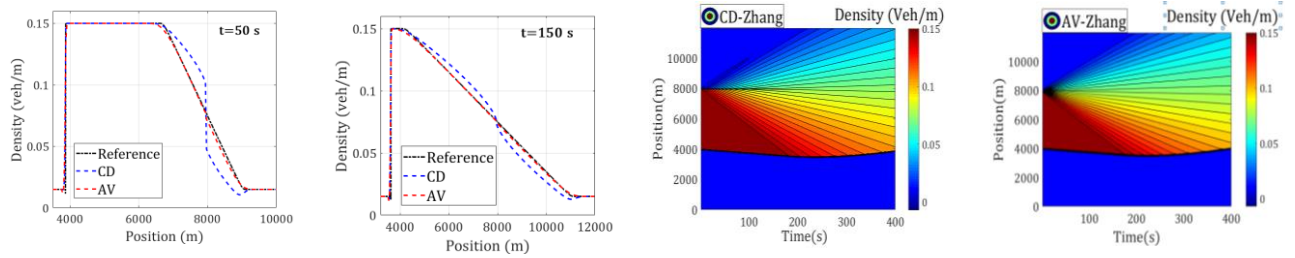
a) Zhang model   b) Zhang model   c) Zhang model   d) Zhang model

1   Fig 5) *Results for case 3. a) Cross section at t=50s, b) Cross section at t=150s, c) CD spatiotemporal*
2   *evolution of local densities, d) AV spatiotemporal evolution of local densities. e) Cross section at*
3   *t=50s, f) Cross section at t=150s, g) CD spatiotemporal evolution of local densities, h) AV*
4   *spatiotemporal evolution of traffic densities.*

5   Case 3 is simply a condition in which free-flow condition is present in the upstream and
6   downstream of congestion regime. Solution of this Riemann problem for the downstream
7   discontinuity is expansion waves heading both to the left and right side because of discontinuous
8   transition from congestion regime to the free-flow condition. Solution of the Riemann problem in
9   the upstream is a shockwave which initially propagates leftwards, and after some points when
10   free-flow condition is provided in downstream, this shockwave heads to the right side. This case
11   cannot be simulated by standard McCormack scheme as discussed before. However, both
12   smoothing methods can overcome oscillations to an acceptable point and produce reasonable
13   results as shown in spatiotemporal evolutions of traffic densities shown in figure 5 (c, d, g, h).
14   Cross-sectional results (fig- 5 (a, b, e, f), show that effects of oscillations are conspicuous when CD
15   method is applied. Spatiotemporal results (fig- 5 (c, d, g, h), however, reveal that there is slight
16   difference in the overall results of CD method compared to AV, which also provides better results
17   in these cases as well.
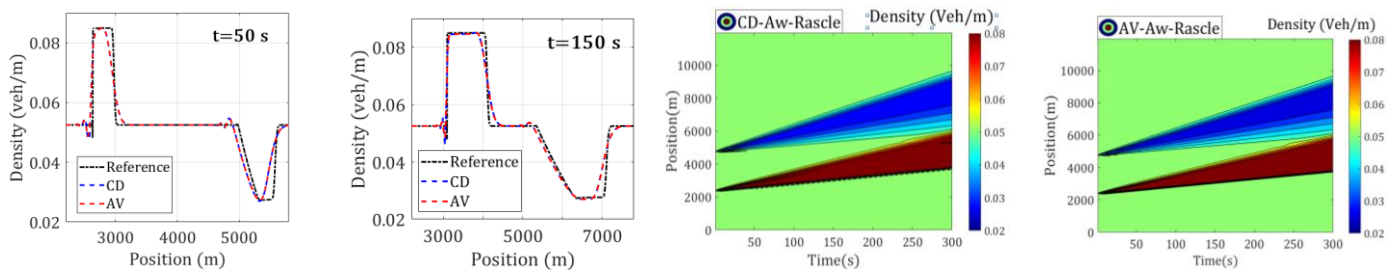
a) Aw-Rascle model   b) Aw-Rascle model   c) Aw-Rascle model   d) Aw-Rascle model
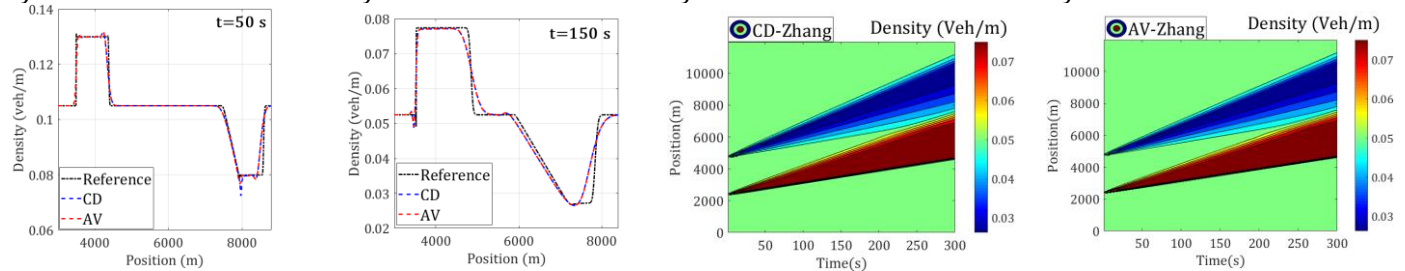
a) Zhang model   b) Zhang model   c) Zhang model   d) Zhang model

18   Fig 6) *case 4. a) cross section at t=50s, b) cross section at t=150s, c) CD spatiotemporal evolution*
19   *of local densities, d) AV spatiotemporal evolution of local densities, e) cross section at t=50s, f) cross*
20   *section at t=150s, g) CD spatiotemporal evolution of local densities, h) AV spatiotemporal evolution*
21   *of traffic densities.*

a) Aw-Rascle model   b) Aw-Rascle model   c) Aw-Rascle model   d) Aw-Rascle model
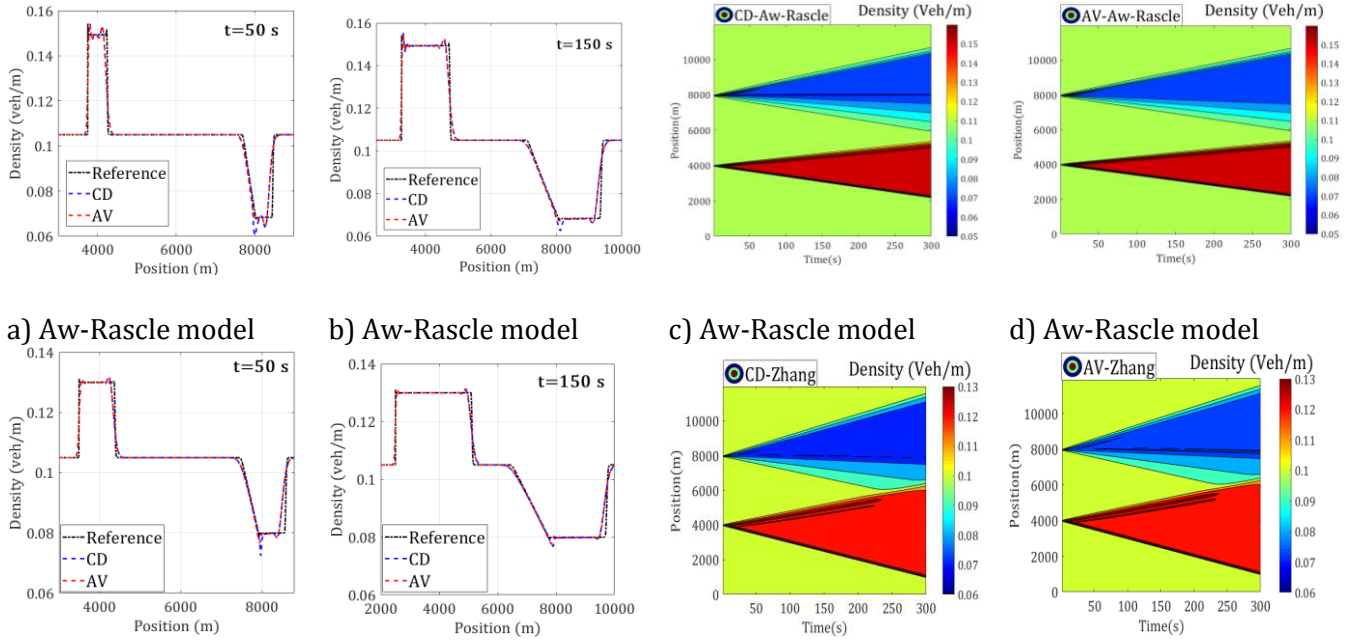
a) Zhang model   b) Zhang model   c) Zhang model   d) Zhang model

1   Fig 7) *Results for case 5. a) Cross section at t=50s, b) Cross section at t=150s, c) CD*
2   *spatiotemporal evolution of local densities, d) AV spatiotemporal evolution of local densities. e) Cross*
3   *section at t=50s, f) Cross section at t=150s, g) CD spatiotemporal evolution of local densities, h) AV*
4   *spatiotemporal evolution of traffic densities.*

5   Simulation of non-equilibrium traffic state has been performed on case 4 and 5. In these test cases,
6   despite initial uniform density profile, local speeds are not in equilibrium with traffic density.
7   Initial traffic density in case 4 represent free-flow condition while in case 5, congestion regime is
8   dominant. Non-equilibrium local speeds results in formation of shock-waves as contact
9   discontinuities in these cases and also expansion waves. Numerical oscillations in standard
10   McCormack lead to the failure of scheme for simulation of such cases. However, both smoothing
11   methods can successfully capture those waves and present reasonable results for spatiotemporal
12   evolution of traffic flow as illustrated in figures 6 and 7.

13   *Results of numerical tests on smoothed McCormack with TVD Runge-Kutta scheme*

14   Figures 3-7 show the test results, for both Aw-Rascle and Zhang model, comparing the smoothing
15   methods with the reference solutions. Both numerical methods show little spurious oscillations,
16   though there are more and stronger oscillations with the Zhang model, and with the CD. This is
17   especially strong in case 2: the Zhang model exhibits more oscillations than the Aw-Rascle model
18   and the AV performs better at reducing them than the CD method. Results also show that the
19   Runge-Kutta time stepping provides a high-order temporal accuracy while avoid numerical
20   oscillations. Cases 2, 3 and 4, furthermore show differences in the continuous parts of the solution
21   as well: i.e. the red (CD) line deviates from the reference solution further than the blue line (AV)
22   does. In fact, cases 1-3 show an almost exact overlap between the AV and the reference solution,
23   except for at discontinuities. Cases 4 and 5 show that AV is also susceptible to diffusion and the
24   numerical solution is smoother than the reference solution. Results also show that the initial
25   instabilities are damped and oscillations decrease over time; this is especially visible in the
26   contour plots for cases 4 and 5 (fig- 6, 7). Finally, the choice of the smoothing parameters
27   influences the results as shown in figure 2, which also indicates that the choice of κ (in AV) is much
28   less sensitive then the choice of S (in CD) in terms of numerical diffusion.

29   **Discussion and Conclusion**

30   Aw-Rascle type traffic flow models are systems of homogeneous non-linear hyperbolic equations.
31   Because of their homogeneity, they require different numerical methods than the non-

`

homogeneous higher-order traffic flow models. More specifically, the standard McCormack spatial integration scheme works fine for non-homogeneous models, but does not for homogeneous ones. Therefore, two smoothing methods are proposed to reduce numerical oscillations inherent to the standard McCormack scheme. Furthermore, it is suggested to apply a TVD Runge-Kutta scheme to increase the order of temporal accuracy. Results show that both Central Dispersion Smoothing and Artificial Viscosity Method lead to more accurate results with less numerical oscillation. Diffusion is kept within reasonable limits in both methods compared to reference solution. Because of better performance at discontinuities (less numerical oscillations) and a lower sensitivity of the smoothing parameter, the Artificial Viscosity Method is preferred.

Future developments include application of the proposed numerical methods in simulation tools. Therefore, the methods will have to be extended to deal with nodes such as on ramps and off ramps. Furthermore, the methods can be studied further and applied to different models, such as other Aw-Rascle type models, the generic second-order model, traffic flow models in Lagrangian formulation and to both first order and higher order models including multiple vehicle classes (e.g. cars and trucks). Non-Homogeneous models with relative small source terms (e.g. due to large relaxation times) will also benefit from applying the smoothing methods in combination with the McCormack and TVD Runge-Kutta schemes. Other types of smoothing, including flux limiting, can be studied and compared with those presented here. Study on other flux limiting terms for smoothing is also suggested for comparison purposes. Accuracy of the methods, as well as their computational costs in terms of memory and computation time can be compared in more detail.

References

[1] D. Helbing, A. Hennecke, V. Shvetsov, M. Treiber, Micro-and macro-simulation of freeway traffic, Mathematical and computer modelling, 35 (2002) 517-547.

[2] D. Helbing, Traffic and related self-driven many-particle systems, Reviews of Modern Physics, 73 (2001) 1067-1141.

[3] T. Seo, A.M. Bayen, T. Kusakabe, Y. Asakura, Traffic state estimation on highway: A comprehensive survey, Annual Reviews in Control, 43 (2017) 128-151.

[4] N. Bellomo, C. Dogbe, On the Modeling of Traffic and Crowds: A Survey of Models, Speculations, and Perspectives, SIAM Review, 53 (2011) 409-463.

[5] S.P. Hoogendoorn, P.H. Bovy, State-of-the-art of vehicular traffic flow modelling, Proceedings of the Institution of Mechanical Engineers, Part I: Journal of Systems and Control Engineering, 215 (2001) 283-303.

[6] M. Treiber, A. Kesting, Traffic flow dynamics, Traffic Flow Dynamics: Data, Models and Simulation, Springer-Verlag Berlin Heidelberg, (2013).

[7] F. van Wageningen-Kessels, H. van Lint, K. Vuik, S. Hoogendoorn, Genealogy of traffic flow models, EURO Journal on Transportation and Logistics, 4 (2015) 445-473.

[8] M. Saifuzzaman, Z. Zheng, Incorporating human-factors in car-following models: A review of recent developments and research needs, Transportation Research Part C: Emerging Technologies, 48 (2014) 379-403.

[9] A.I. Delis, I.K. Nikolos, M. Papageorgiou, Macroscopic traffic flow modeling with adaptive cruise control: Development and numerical solution, Computers & Mathematics with Applications, 70 (2015) 1921-1947.

[10] M. Treiber, A. Kesting, Macroscopic Models with Dynamic Velocity, in: Traffic Flow Dynamics: Data, Models and Simulation, Springer Berlin Heidelberg, Berlin, Heidelberg, 2013, pp. 127-155.

[11] J. Treiterer, J. Myers, The hysteresis phenomenon in traffic flow, Transportation and traffic theory, 6 (1974) 13-38.

[12] J.A. Laval, Hysteresis in the fundamental diagram: impact of measurement methods, in: Transportation Research Board 89th Annual Meeting, 2010.

[13] D. Chen, S. Ahn, Z. Zheng, J. Laval, Traffic Hysteresis and the Evolution of Stop-and-Go Oscillations, in: Transportation Research Board 92nd Annual Meeting, 2013.

`

[14] K. Yuan, V.L. Knoop, L. Leclercq, S.P. Hoogendoorn, Capacity drop: a comparison between stop-and-go wave and standing queue at lane-drop bottleneck, Transportmetrica B: Transport Dynamics, 5 (2017) 145-158.

[15] C. Tampere, S. Hoogendoorn, B. van Arem, A Behavioural Approach to Instability, Stop and Go Waves, Wide Jams and Capacity Drop, Transportation and traffic theory, 16 (2005) 205-228.

[16] M. Saifuzzaman, Z. Zheng, M.M. Haque, S. Washington, Understanding the mechanism of traffic hysteresis and traffic oscillations through the change in task difficulty level, Transportation Research Part B: Methodological, 105 (2017) 523-538.

[17] R.J. LeVeque, Finite volume methods for hyperbolic problems, Cambridge university press, 2002.

[18] G. Witham, Linear and Non-linear Waves John Wiley, New York, (1974).

[19] H.J. Payne, Models of freeway traffic and control, Mathematical models of public systems, (1971).

[20] B.S. Kerner, P. Konhäuser, Structure and parameters of clusters in traffic flow, Physical Review E, 50 (1994) 54.

[21] M. Treiber, A. Hennecke, D. Helbing, Derivation, properties, and simulation of a gas-kinetic-based, nonlocal traffic model, Physical Review E, 59 (1999) 239-253.

[22] A. Aw, M. Rascle, Resurrection of" second order" models of traffic flow, SIAM journal on applied mathematics, 60 (2000) 916-938.

[23] H.M. Zhang, A non-equilibrium traffic model devoid of gas-like behavior, Transportation Research Part B: Methodological, 36 (2002) 275-290.

[24] C.F. Daganzo, Requiem for second-order fluid approximations of traffic flow, Transportation Research Part B: Methodological, 29 (1995) 277-286.

[25] F. van Wageningen-Kessels, B. van't Hof, S.P. Hoogendoorn, H. Van Lint, K. Vuik, Anisotropy in generic multi-class traffic flow models, Transportmetrica A: Transport Science, 9 (2013) 451-472.

[26] J.-P. Lebacque, S. Mammar, H. Haj-Salem, The Aw–Rascle and Zhang's model: Vacuum problems, existence and regularity of the solutions of the Riemann problem, Transportation Research Part B: Methodological, 41 (2007) 710-721.

[27] D. Helbing, M. Treiber, Numerical simulation of macroscopic traffic equations, Computing in Science & Engineering, 1 (1999) 89-99.

[28] J.-P. Lebacque, S. Mammar, H.H. Salem, Generic second order traffic flow modelling, in: Transportation and Traffic Theory 2007. Papers Selected for Presentation at ISTTT17, 2007.

[29] R. Abgrall, J. Qiu, Preface to the special issue "High order methods for CFD problems", Journal of Computational Physics, 230 (2011) 4101-4102.

[30] A.I. Delis, I.K. Nikolos, M. Papageorgiou, High-resolution numerical relaxation approximations to second-order macroscopic traffic flow models, Transportation Research Part C: Emerging Technologies, 44 (2014) 318-349.

[31] D. Ngoduy, R. Liu, Multiclass first-order simulation model to explain non-linear traffic phenomena, Physica a-Statistical Mechanics and Its Applications, 385 (2007) 667-682.

[32] J.C. Tannehill, D.A. Anderson, R.H. Pletcher, Computational fluid mechanics and heat transfer, Taylor & Francis, (1997).

[33] A. Jameson, W. Schmidt, E. Turkel, Numerical solutions of the Euler equations by finite volume methods using Runge-Kutta time-stepping schemes, AIAA paper, 1259 (1981) 1981.

[34] C.-W. Shu, S. Osher, Efficient implementation of essentially non-oscillatory shock-capturing schemes, Journal of Computational Physics, 77 (1988) 439-471.

[35] B. Greenshields, W. Channing, H. Miller, A study of traffic capacity, in: Highway research board proceedings, National Research Council (USA), Highway Research Board, 1935.

[36] R.J. LeVeque, Finite difference methods for ordinary and partial differential equations: steady-state and time-dependent problems, Siam, 2007.

[37] E.F. Toro, Riemann solvers and numerical methods for fluid dynamics: a practical introduction, Springer Science & Business Media, 2013.

[38] W.-Y. Tan, Shallow water hydrodynamics: Mathematical theory and numerical solution for a two-dimensional system of shallow-water equations, Elsevier, 1992.

`

[39] P. Garcia-Navarro, F. Alcrudo, J. Saviron, 1-D open-channel flow simulation using TVD-McCormack scheme, Journal of Hydraulic Engineering, 118 (1992) 1359-1372.

[40] M. Sun, K. Takayama, Conservative smoothing on an adaptive quadrilateral grid, Journal of Computational Physics, 150 (1999) 143-180.

[41] R.C. Swanson, E. Turkel, On central-difference and upwind schemes, Journal of computational physics, 101 (1992) 292-306.

[42] C.F. Daganzo, A variational formulation of kinematic waves: basic theory and complex boundary conditions, Transportation Research Part B: Methodological, 39 (2005) 187-196.

[43] J.A. Laval, L. Leclercq, The Hamilton–Jacobi partial differential equation and the three representations of traffic flow, Transportation Research Part B: Methodological, 52 (2013) 17-30.